

Microscopic theory of normal liquid ^3He

N. Nafari

*Atomic Energy Organization of Iran, Centre for Theoretical Physics and Mathematics, P.O. Box 11365-8486, Tehran, Iran
and International Centre for Theoretical Physics, P.O. Box 586, 34100 Trieste, Italy*

A. Doroudi

*Atomic Energy Organization of Iran, Centre for Theoretical Physics and Mathematics, P.O. Box 11365-8486, Tehran, Iran
and Department of Physics, Amir-Kabir University, Tehran, Iran*

(Received 8 December 1994)

We have used the self-consistent scheme proposed by Singwi, Tosi, Land, and Sjölander to study the properties of normal liquid ^3He . By employing the Aziz potential (i.e., the Hartree-Fock repulsion plus damped dispersion with an additional parameter) and some other realistic pairwise interactions, we have calculated the static structure factor, the pair-correlation function, the zero-sound frequencies as a function of wave vector, and the Landau parameter F_0^s for different densities. Our results show considerable improvement over the Ng-Singwi model potential of a hard core plus an attractive tail. Agreement between our results and the experimental data for the static structure factor and the zero-sound frequencies is fairly good.

I. INTRODUCTION

The theory of normal liquid ^3He begins with the work of Landau, who introduced the concept of quasiparticle interactions.¹⁻³ The Landau parameters entering the expansion of the free energy specify the strength of the quasiparticle interactions and are to be determined by experiment. Greywall,⁴ Wheatley,⁵ and Alvesalo, Haavasoja, and Manninen⁶ have measured the Landau parameters F_0^s , F_1^a , and F_1^s . The discrepancies among their results are due to experimental uncertainties in the effective-mass ratio, namely, the uncertainties in the measurement of $\lim C(T)/T$ as $T \rightarrow 0$, where $C(T)$ is the specific heat.

One of the aims of any microscopic theory is to calculate these phenomenological parameters from first principles and compare them with the corresponding experimental values. Furthermore, such a theory should provide an understanding of the spectrum of elementary excitations and collective (zero-sound) modes. As for the techniques, these microscopic theories generally rely upon perturbation expansions, computational methods, and nonperturbative approximations.

The perturbative techniques are suited for systems characterized by small parameters. However, real liquid ^3He , due to its high density and strong interactions between its particles, does not possess such parameters. As a result, the perturbative techniques are inappropriate.

On the other hand, numerical techniques such as correlated basis functions⁷ and the Green's function Monte Carlo method⁸ rely heavily on extensive computations. In this paper we use the well-known nonperturbative Singwi, Tosi, Land, and Sjölander (STLS) scheme which is in the form of the generalized random-phase approximation (RPA) with no free parameters. This approximation was originally devised to treat electron correlations at metallic densities,⁹ and in recent years has been applied to a model system of interacting Fermi particles by Ng and Singwi.¹⁰ These authors employ a simple model

potential having a repulsive core and an attractive tail intended to simulate liquid ^3He . Also, in another paper, Niklasson and Singwi¹¹ have studied the neutral Fermi liquid whose particles interact via a Lennard-Jones (LJ) (6,12) potential with a cut at a point inside the core region. The response function used in their STLS scheme resembles the one suggested by Aldrich and Pines,^{12,13} who introduced the polarization potential theory.

Singwi and his collaborators in Refs. 10 and 11 have calculated various physical quantities and obtained qualitative agreement with experiment. However, in order to obtain quantitative agreement with experiment two modifications must be introduced. First, in place of the simple model potential of Ref. 10 a more realistic two-body bare potential must be used. Secondly, the STLS scheme is a long-wavelength approximation and its results in the large- k (small- r) limit are not reliable. In fact, our calculations show that the unphysical results obtained for the radial pair-correlation function inside the core region¹⁰ persist in the presence of more realistic potentials, although they are somewhat softened. In this paper we will address the first part, i.e., the use of a more realistic potential, and leave the modification of the STLS scheme for a future publication.

A realistic two-body potential between closed-shell helium atoms must have a short-range repulsive part due to the Pauli exclusion principle and a long-range attractive tail due to multipole interactions. One of the popular two-body potentials used in the theoretical investigations of liquid helium has been the LJ (6,12) potential. The two parameters entering the LJ (6,12), i.e., the hard-core radius and the well depth, were determined by de Boer and Michels¹⁴ from the second virial coefficients. However, this potential has a few serious drawbacks. First, on theoretical grounds, it is now well understood that the repulsive part of the He-He interaction is best described by a simple exponential.¹⁵ This is supported by He-He scattering experiments as well as transport

coefficient measurements. Secondly, the attractive part of LJ (6,12) includes only the dipole-dipole interaction and does not account for higher multipole terms.

As a result, a number of authors^{16–19} have tried to examine other potentials which have proper asymptotic behavior in the short- and long-range limits and have determined parameters introduced in the pairwise potentials by fitting to the selected second virial coefficient and/or to transport properties such as thermal conductivities and viscosity data. Realistic potentials which satisfy the above-mentioned criteria and agree with many of the experimental data are the Aziz *et al.* potentials^{17,18} and the Fourier-transformable Morse potential of Bruch and McGee.¹⁹

In this paper, by starting with the self-consistent STLS scheme and employing these realistic potentials, we have calculated the static structure factor, the pair-correlation function, the zero-sound frequencies, and the Landau parameters. Furthermore, the variations of these quantities with pressure have been investigated. These calculations show definite improvements over the results of Ng and Singwi's model potential.

The outline of this paper is as follows. In Sec. II we present the STLS scheme and the theoretical framework of our calculations. Section III is devoted to the form of the realistic potentials used in this paper for calculating various physical quantities. We then compare the results obtained for various potentials with the experimental data and with the results cited in Ref. 10. Finally, in Sec. IV we investigate how various pairwise potentials introduced in Refs. 16–19 satisfy the virial theorem, and make some concluding remarks.

II. THEORETICAL FRAMEWORK AND THE STLS SCHEME

Several years ago, Singwi, Tosi, Land, and Sjölander presented a theory of the dielectric formalism⁹ of an electron liquid in the metallic density range ($2 \leq r_s \leq 6$). Analogous to the hierarchy of the Bugoliubov-Born-Green-Kirkwood-Yvon (BBGKY) equations in classical nonequilibrium statistical mechanics, an infinite set of equations of motion for density matrices or alternatively for the Wigner distribution functions can be derived. The central problem in both classical and quantum cases has been that of finding an approximation for breaking the hierarchy of these equations. In the STLS approximation, one sets the two-particle density-density correlation equal to the product of the densities times the static pair-correlation function,

$$\langle \rho(\mathbf{r}, t) \rho(\mathbf{r}', t) \rangle_c = \langle \rho(\mathbf{r}, t) \rangle \langle \rho(\mathbf{r}', t) \rangle [g(\mathbf{r}, \mathbf{r}') - 1], \quad (1)$$

and obtains an equation for the one-particle density matrix $\langle \psi_\sigma^\dagger(\mathbf{r}, t) \psi_\sigma(\mathbf{r}', t) \rangle$. $\psi_\sigma^\dagger(\mathbf{r}, t)$ and $\psi_\sigma(\mathbf{r}, t)$ are the creation and annihilation field operators for an electron with spin σ at space-time coordinates (\mathbf{r}, t) . They then find the following expression for the wave-number- and frequency-dependent density-density response function:

$$\chi_d(k, \omega) = \frac{\chi_0(k, \omega)}{1 - v_{\text{eff}}^s(k) \chi_0(k, \omega)}. \quad (2)$$

$\chi_0(k, \omega)$ is the Lindhard function and $v_{\text{eff}}^s(k)$ is the static effective spin-symmetric particle-hole interaction. Equation (2) is in the form of the generalized random-phase approximation and can be reduced to the RPA if $v_{\text{eff}}^s(k)$ is replaced by the Fourier transform of the bare potential between pairs of particles. For an isotropic system, the effective quasiparticle interaction within the STLS scheme is given in terms of the pair-correlation function $g(r)$ by

$$v_{\text{eff}}^s(r) = - \int_r^\infty dr g(r) \frac{dv(r)}{dr}. \quad (3)$$

Here $v(r)$ is the bare potential between pairs of particles. The Fourier transform of $v_{\text{eff}}^s(r)$, by definition, reduces to

$$v_{\text{eff}}^s(k) = - \frac{4\pi}{k^3} \int_0^\infty dr g(r) \frac{dv(r)}{dr} [\sin(kr) - kr \cos(kr)]. \quad (4)$$

Through the *fluctuation-dissipation* theorem which relates the imaginary part of the inverse of the dielectric function to the dynamical structure factor $S(k, \omega)$, and through the relation between the density-density response function $\chi_d(k, \omega)$ and the dielectric function, the following exact relation between the static structure factor $S(k)$ and the imaginary part of $\chi_d(k, \omega)$ can be shown:

$$S(k) = \int_{-\infty}^{+\infty} \frac{d\omega}{2\pi} S(k, \omega) = - \frac{3\pi}{k_f^3} \int_{-\infty}^{+\infty} d\omega \text{Im} \chi_d(k, \omega). \quad (5)$$

Finally, for an isotropic system, the pair-correlation function and the static structure factor are related by

$$g(r) = 1 + \frac{3}{2rk_f^3} \int_0^\infty dk k \sin(kr) [S(k) - 1]. \quad (6)$$

We solve the set of equations (2), (4), (5), and (6) iteratively. By starting with the known expression for $g(r)$ in the Hartree-Fock approximation, we use Eqs. (4), (2), (5), and (6) successively to obtain the new $g(r)$. Then the iterative process is continued until convergence is achieved.

Note that, in contrast to the variational or Monte Carlo methods used by different authors,^{7,8} this iterative process can be carried out on ordinary personal computers.

III. TWO-BODY INTERACTIONS AND RESULTS

In our numerical work, we have used the HFD-B potential of Aziz, McCourt, and Wong¹⁸ and the MDD-2 Morse potential of Bruch and McGee.¹⁹ The analytical form of the HFD-B potential is

$$v(r) = \epsilon \left[A^* \exp(-\alpha^* x + \beta^* x^2) - f(x) \sum_{j=0}^2 c_{2j+6} / x^{2j+6} \right], \quad (7)$$

where

$$f(x) = \begin{cases} \exp\left[-\left(\frac{D}{x}-1\right)^2\right] & \text{if } x < D, \\ 1 & \text{if } x \geq D. \end{cases}$$

Here, $x = r/r_m$, where $r_m = 2.963 \text{ \AA}$ and $\epsilon/k_B = 10.948 \text{ K}$, k_B being the Boltzmann factor. The values of dispersion coefficients, $c_6 = 1.36745214$, $c_8 = 0.42123807$, and $c_{10} = 0.17473318$, are taken from the *ab initio* calculations of Thakkar and Koide, Meath, and Allnatt.²⁰ The other parameters appearing in this potential are $A^* = 184431.01$, $\alpha^* = 10.43329537$,

$$v(r) = \begin{cases} -\epsilon\{2\exp[c(1-r/r_m)] - \exp[2c(1-r/r_m)]\} & \text{if } r \leq r_s, \\ -(c_6 r^{-6} + c_8 r^{-8}) & \text{if } r \geq r_s. \end{cases} \quad (8)$$

The dispersion coefficients were the best available at the time ($c_6 = 10213.8 \text{ K \AA}^6$ and $c_8 = 27671.4 \text{ K \AA}^8$). The well depth is $\epsilon = 10.75 \text{ K}$, and the other parameters are $r_m = 3.0238 \text{ \AA}$, $c = 6.12777$, and $r_s = 3.68280 \text{ \AA}$. This potential, also, has the correct asymptotic behavior with continuous derivative at r_s . Its parameters are chosen to agree with thermodynamic data to within a few percent.

Without cutting off these potentials in the core region ($2.15 < r_c < 2.3 \text{ \AA}$), our iterative procedure would not converge. However, the results obtained in this way did not sensitively depend on the position of the cutoff point r_c . The cutoff point used in this paper is $r_c = 2.22 \text{ \AA}$ with $v(r_c) = 162.75 \text{ K}$ for the HFD-B potential and $r_c = 2.20 \text{ \AA}$ with $v(r_c) = 188.87 \text{ K}$ for the MDD-2 potential.

This lack of convergence has its origin in the STLS scheme and not in the way our numerical procedure is carried out. The integrand of the right-hand side of Eq. (4) contains a product of the pair-correlation function $g(r)$ and the radial derivative of the bare potential between two helium atoms, i.e., $dv(r)/dr$. Since this derivative diverges rapidly for small r values, $g(r)$ must assume vanishingly small values in the core region for, otherwise, $v_{\text{eff}}^s(k)$ will not remain finite.²⁵ On the other hand, the STLS scheme contains no inherently built-in mechanism through which the pair-correlation function could assume vanishingly small values for small r . Indeed, the values of $g(0)$ obtained through the STLS scheme are generally finite (see Fig. 3 of this paper and Fig. 3 of Ref. 9) and by continuity must remain finite near the origin. Cutting the potential at r_c and replacing the core values by a constant is equivalent to setting the integrand of Eq. (4) equal to zero in that region. The neglect of the contribution of the integrand inside the core region could also be obtained by bringing in the physical assumption of vanishing $g(r)$ in that region in each iteration. Another way of overcoming this difficulty is to calculate the pair-correlation function outside the core region by the STLS scheme and join it smoothly to its theoretically known expression, i.e., $g(r) = A \exp(-b/r^5)$,²⁶ in the core region. Our numerical results show that, although the pair-correlation function obtained in this way is some-

$\beta^* = -2.27965105$, and $D = 1.4826$. This potential has been fitted to low-temperature second-virial-coefficient data²¹ and to accurate room-temperature viscosity data.²² Moreover, by pinning its repulsive wall value to that calculated by Ceperley and Partridge²³ at one bohr, the authors made this potential less repulsive than that of Ref. 17, and obtained excellent agreement with the experimental data inferred from high-energy integral-cross-section measurement.²⁴

Next we will discuss the MDD-2 Morse potential of Bruch and McGee.¹⁹ This Fourier-transformable potential is defined as

what closer to experiments^{27,28} than the $g(r)$ presented in this paper, the resulting structure factor for small k values becomes unphysical. For these reasons, we have introduced the cutoff discussed above as a way of avoiding the small- r problem in the STLS scheme.

For studying the pressure dependence of the physical quantities, we have repeated our calculations for different densities. The density enters the theory through the known relation $3\pi^2 n = k_f^3$, where k_f is the Fermi wave vector. The different pressures used in this paper are 0, 6, 17, and 35 atm and their corresponding densities in units of 10^{-28} m^{-3} are, respectively, 1.64, 1.88, 2.12, and 2.36.

In the following subsections we will present our results.

A. The static structure factor

Figure 1 shows the results of our self-consistent calculations of the static structure factor $S(k)$ using the HFD-B potential for three different densities of 1.5, 1.64, and 1.88 in units of 10^{-28} m^{-3} . As expected, in moving

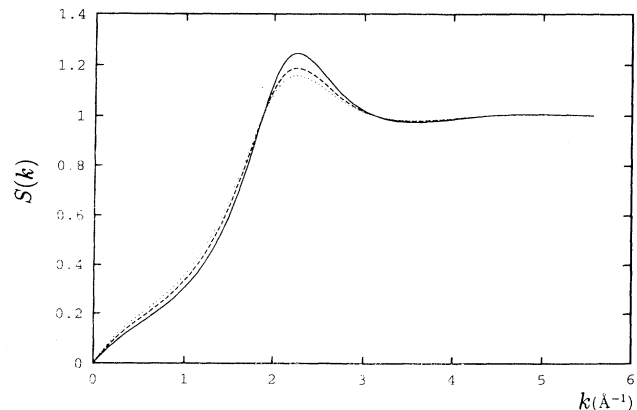


FIG. 1. Static structure factor $S(k)$ vs k for three different densities. The three curves from bottom to top correspond to the densities 1.5, 1.64, and 1.88 in units of 10^{-28} m^{-3} , respectively.

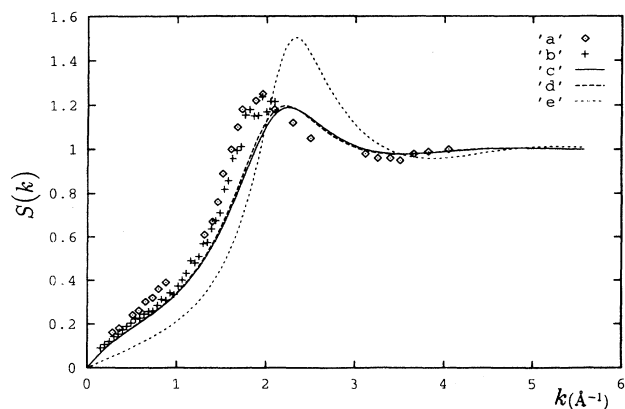


FIG. 2. Calculated static structure factor $S(k)$ at saturated vapor pressure (SVP) compared with experiment. The solid line (curve *c*) refers to the Aziz *et al.* potential (HFD-B), the dashed line (curve *d*) refers to the potential of Bruch and McGee (MDD-2), and the short-dashed line (curve *e*) represents the results of Ng and Singwi's model potential of Ref. 10 for the parameter $c=1.8$. The plus signs and dotted diamonds represent the experimental data of Refs. 25 and 26, respectively.

towards higher pressures (higher densities), the peak height in Fig. 1 increases, but the variation of peak position with pressure is negligible. In Fig. 2, we compare our calculated $S(k)$ at the normal density of 1.64×10^{-28} atom m^{-3} using HFD-B and MDD-2 potentials with the corresponding experimental data of Hallock²⁷ and Achter and Meyer.²⁸ For comparison purposes, the calculation of Ng and Singwi¹⁰ for the same density is also shown.

The realistic potentials of HFD-B and MDD-2 yield results very close to each other and in good agreement with the experimental data. However, the calculated peak positions are shifted towards larger k values relative to their experimental counterparts. This could be an artifact of the STLS approximation, which is expected to depart from exact results at the short-wavelength limit. We believe the inclusion of three-body interactions will bring about further improvements. All three potentials show a plateaulike structure at small wave-vector values. This behavior, which is consistent with the experimental findings of Refs. 27 and 28 for liquid ^3He , is related to the behavior of these potentials outside the core region. As Ng and Singwi mention in their paper,¹⁰ such plateaulike behavior appears when an attractive tail is added to a hard-core potential.

Comparison of our calculated structure factor with the variational results of Viviani *et al.*²⁹ shows that we have obtained closer agreement with experiment^{27,28} for the small k values. For instance, the experimental plateaulike behavior does not appear in these authors' theoretical calculations. As is expected, their peak position and large- k behavior of $S(k)$ are somewhat closer to experiment than ours.

B. Pair-correlation function

The self-consistent calculations of the pair-correlation function $g(r)$ for three different densities are shown in

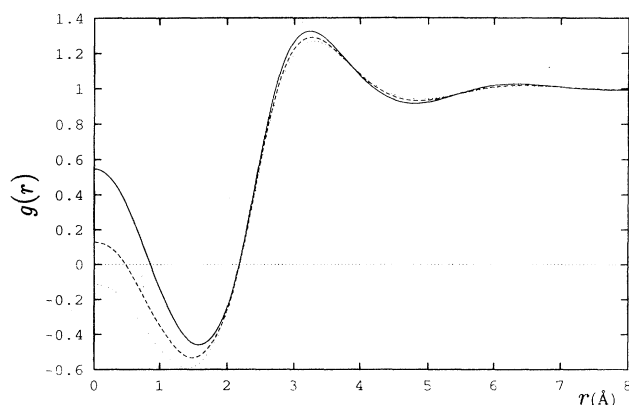


FIG. 3. Pair-correlation function $g(r)$ vs r for three different densities as specified in Fig. 1.

Fig. 3. Using the Aziz *et al.* potential as the bare pairwise potential, our calculated $g(r)$ outside the core region is reasonable, and its peak height is in good agreement with experiment.

Figure 4 shows the comparison of our calculated $g(r)$ with the experimental data of Achter and Meyer,²⁸ and with the results based on Ref. 10 in the region outside the core. However, inside the core region, $g(r)$ oscillates and assumes negative values. This unphysical behavior is even more pronounced when we use the MDD-2 or the Ng-Singwi model potential. This is again an artifact of the STLS approximation in the large- k limit.

Comparison of our pair-correlation function outside the core region with the variational results of Viviani *et al.*²⁹ shows that our calculated $g(r)$ is not as close to the experimental findings of Achter and Meyer²⁸ as the $g(r)$ calculated by Viviani *et al.* However, our calculated pair-correlation function shows better agreement with ex-

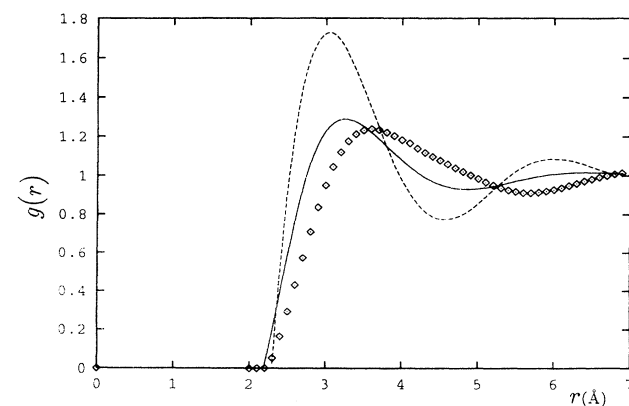


FIG. 4. Calculated pair-correlation function $g(r)$ using the Aziz *et al.* potential at SVP (solid line) compared with the result of the Ng-Singwi model potential of Ref. 10 for the parameter $c=1.8$ (dashed line) and with the experimental data of Ref. 26 (dotted diamonds).

periment as compared with the theoretical results of Buchan and Clark.³⁰ In particular, the peak height of $g(r)$ obtained in this paper is closer to the experimental results. We think that modification of the STLS scheme, namely, modification of the field correction factor, will improve our results and will make them comparable with other theoretical investigations.

C. The zero-sound dispersion

Zero-sound modes in liquid ^3He , as predicted by Landau,¹ are the high-frequency modes of vibration of the Fermi surface. To obtain the zero-sound dispersion frequencies, one sets the denominator of the density-density response function $\chi_d(k, \omega)$, equal to zero, i.e.,

$$1 - v_{\text{eff}}^s(k) \chi_0(k, \omega) = 0. \quad (9)$$

The roots of this equation give the zero-sound frequencies as a function of the wave vector k . The results of our calculations at zero pressure (SVP) using the MDD-2 and Aziz *et al.* potentials are shown in Fig. 5. Here, for the purpose of comparison, we have also reproduced results of the model potential of Ref. 10 and the experimental data of Ref. 31 for liquid ^3He . Again, the results of the MDD-2 and the Aziz *et al.* potentials, as shown in Fig. 5, are nearly the same, and closer to the experimental data than those of Ref. 10.

Other theoretical works, such as the polarization potential theory of Aldrich and Pines¹² for obtaining the dispersion curve, have resulted in excellent agreement between theory and experiment. However, we should remind the reader that our theoretical scheme is parameter-free, depending only on the bare potential between two helium atoms, whereas the parameters of the phenomenological theory of Aldrich and Pines are obtained by fitting to the comparatively high-momentum-

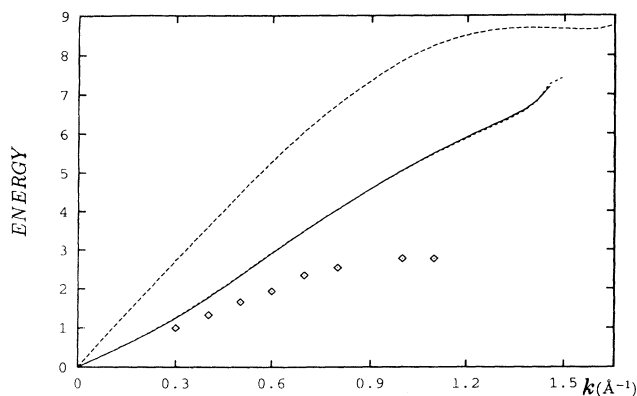


FIG. 5. Calculated dispersion curve for the Aziz *et al.* potential (HFD-B) at SVP (solid line) compared with the experimental data of Ref. 27 (dotted diamonds) and with the result of the Ng-Singwi model potential of Ref. 10 for the parameter $c=1.8$ (dashed line). The short-dashed line which almost coincides with the dispersion curve for the Aziz *et al.* potential is the result of the MDD-2 potential. Energy is given in units of $\hbar^2 k_f^2 / 2m$.

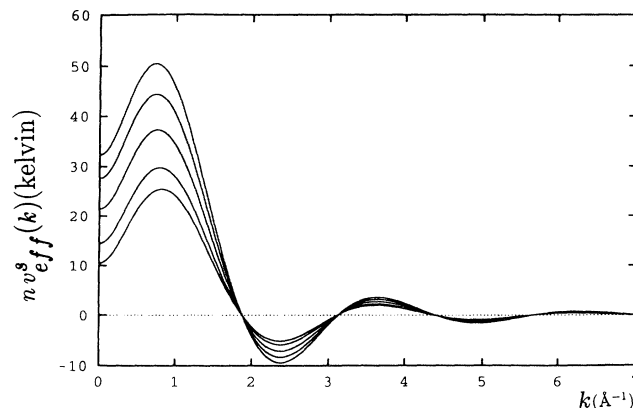


FIG. 6. $nv_{\text{eff}}^s(k)$ in kelvin vs k for five different densities. The five curves from bottom to top correspond to the densities 1.5, 1.64, 1.88, 2.12, and 2.36 in units of 10^{-28} m^{-3} .

transfer neutron scattering data and by satisfying the moment sum rules.

D. The effective potential and the Landau parameter F_0^s

The calculated effective potential $nv_{\text{eff}}^s(k)$ for five different densities is shown in Fig. 6. The bare pairwise potential used in here is that of Aziz *et al.* Results for zero pressure (SVP) are similar, and in agreement with those obtained in the polarization potential theory of Aldrich and Pines.^{12,13} The other potentials yield similar results.

The Landau parameter F_0^s is obtained by using the relation

$$F_0^s = \frac{3}{2} \frac{m^*}{m} \lim_{k \rightarrow 0} [nv_{\text{eff}}^s(k)]. \quad (10)$$

m^* is the effective mass of ^3He quasiparticles. For ratios of m^*/m , we have used the experimental data of Ref. 4. Calculated values of the Landau parameter F_0^s for different pressures are given in Table I. For comparison purposes, the experimental values of F_0^s as given in Ref. 4 are also shown.

TABLE I. Comparison between the calculated Landau parameter F_0^s and the experimental values for different densities.

Density (10^{-28} m^{-3})	F_0^s (calculated)	F_0^s (expt.)
1.5		
1.64	11.9	9.2
1.88	20.2	22.2
2.12	31.5	45.8
2.36	43.9	87.09

TABLE II. Ground-state energy of liquid ^4He for different two-body interactions.

Potential	Symbol	E_{GS} (K)
Morse potential of Bruch and McGee	MDD-2	-19.01
Frost-Musulin potential of Bruch and McGee	FDD-1	-13.89
Modified Frost-Musulin	MFM	-14.81
Lennard-Jones	LJ (6,12)	-1.05
Aziz <i>et al.</i> (1979)	HFDHE2	-12.95
Aziz, McCourt, and Wong (1987)	HFD-B	-12.90

IV. DISCUSSION AND CONCLUDING REMARKS

Here we have used the STLS approximation and have calculated the static structure factor, the pair-correlation function, the zero-sound frequencies, and the Landau parameter F_0^s as a function of pressure. The realistic pairwise potentials employed in this paper are those of Aziz *et al.* and Bruch and McGee. These potentials have the correct asymptotic behavior and are fitted to various thermodynamic data.

Following Sposito,³² we have tried to see how well these potentials satisfy the virial theorem and consequently the relation for the ground-state energy E_{GS} for liquid ^4He , i.e.,

$$E_{\text{GS}} = \frac{1}{4}n \int g(\mathbf{r})[\mathbf{r} \cdot \nabla v(\mathbf{r}) + 2v(\mathbf{r})]d\mathbf{r}. \quad (11)$$

Here n is the density, $g(\mathbf{r})$ is the pair-correlation function, and $v(\mathbf{r})$ is the interaction potential between pairs of particles.

The experimental value of the ground-state energy per ^4He atom according to Ref. 33 is about -6 to -7 K. We have calculated the right-hand side (RHS) of Eq. (11) using the HFD-B, MDD-2, LJ (6,12), and some of the Fourier-transformable potentials presented in Ref. 16. Table II shows the calculated values of the RHS of Eq. (11).

In this calculation, we used the Achter and Meyer²⁸ experimental data for the pair-correlation function and benefited from the Weddle rule and spline integration techniques. [$g(r)$ was assumed to be 1 beyond $r = 10 \text{ \AA}$.]

The comparison of the numbers appearing in Table II with their experimental counterparts, i.e., -6 to -7 K, shows that the Aziz *et al.* potential is the best among the ones considered here. This is in agreement with the sup-

port given by other experimental data mentioned earlier. In passing, we would like to point out that the well depths of the HFD-B and MDD-2 potentials used in our calculations lie in the expected range of 10.7 ± 0.4 K predicted by Ref. 34.

As mentioned earlier, our main purpose in this paper was to examine improvements brought about by the use of realistic potentials. Overall, there is good agreement between the theory based on the original form of the STLS scheme and the experimental data in the long-wavelength (large- r) limit. The agreement between the calculated static structure factor and experiments is good over a wider range of k values. However, as expected, the pair-correlation function becomes unphysical in the core region. Also, the zero-sound frequencies in the large- k region deviate appreciably from experimental data.

These discrepancies are partially due to the neglect of the three-body interactions which play an important role in treating liquid ^3He . We believe that generalization of the STLS approximation to a frequency-dependent field correction factor as well as the inclusion of three-body interactions will improve our results and bring about better agreement between this formalism and experiment.

ACKNOWLEDGMENTS

One of the authors (N.N.) is grateful to the late Professor K. S. Singwi for his guidance and would like to thank Dr. G. Vignale for interesting discussions and hospitality provided at the University of Missouri, Columbia. He would also like to thank Professor Abdus Salam, the International Atomic Energy Agency, and UNESCO for hospitality at the International Centre for Theoretical Physics, Trieste.

¹L. D. Landau, *Sov. Phys. JETP* **5**, 101 (1957).

²D. Pines and P. Nozières, *The Theory of Quantum Liquids* (Benjamin, New York, 1966), Vol. 1.

³G. Baym and C. Pethick, *Landau Fermi Liquid Theory* (Wiley, New York, 1991).

⁴D. S. Greywall, *Phys. Rev. B* **27**, 2747 (1983).

⁵J. C. Wheatley, *Rev. Mod. Phys.* **47**, 415 (1975).

⁶T. A. Alvesalo, T. Haavasoja, and M. T. Manninen, *J. Low Temp. Phys.* **45**, 373 (1981).

⁷E. Krotscheck, J. W. Clark, and A. D. Jackson, *Phys. Rev. B* **28**, 5088 (1983).

⁸D. M. Ceperley and M. H. Kalos, in *Monte Carlo Methods in Statistical Physics*, edited by K. Binder, Topics in Current Physics Vol. 7 (Springer-Verlag, Berlin, 1979), Chap. 4.

⁹K. S. Singwi, M. P. Tosi, R. H. Land, and A. Sjölander, *Phys. Rev.* **176**, 589 (1968); K. S. Singwi and M. P. Tosi, *Solid State Phys.* **36**, 177 (1981), and references therein.

¹⁰Tai Kai Ng and K. S. Singwi, *Phys. Rev. B* **35**, 1708 (1987); **35**, 6683 (1987).

¹¹G. Niklasson and K. S. Singwi, *Solid State Commun.* **59**, 575 (1986).

¹²C. H. Aldrich III and D. Pines, *J. Low Temp. Phys.* **32**, 689

- (1978).
- ¹³D. Pines, in *Highlight of Condensed Matter Theory*, Proceedings of the International School of Physics "Enrico Fermi," Course LXXX-IX Varena, Italy, edited by F. Bassani *et al.* (North-Holland, Amsterdam, 1985), pp. 580–643.
- ¹⁴J. de Boer and A. Michels, *Physica* **6**, 409 (1939).
- ¹⁵R. B. Bernstein and J. T. Mucherman, in *Intermolecular Forces*, edited by J. O. Hirschfelder (Wiley, New York, 1967); P. Bertoncini and A. C. Wahl, *Phys. Rev. Lett.* **25**, 991 (1970).
- ¹⁶R. F. Bishop, H. B. Ghassib, and M. R. Strayer, *J. Low Temp. Phys.* **26**, 669 (1977).
- ¹⁷R. A. Aziz *et al.*, *J. Chem. Phys.* **70**, 4330 (1979).
- ¹⁸R. A. Aziz, F. R. W. McCourt, and C. C. K. Wong, *Mol. Phys.* **61**, 1487 (1987).
- ¹⁹L. W. Bruch and I. J. McGee, *J. Chem. Phys.* **46**, 2959 (1967); **52**, 5884 (1970).
- ²⁰A. Thakkar, *J. Chem. Phys.* **75**, 4496 (1981); A. Koide, W. J. Meath, and A. R. Allnatt, *J. Phys. Chem.* **86**, 1222 (1982).
- ²¹F. C. Maticotta, G. T. McConville, P. P. M. Steur, and M. Durieux, *Metrologia* **24**, 61 (1987).
- ²²E. Vogel, *Ber. Bunsenges. Phys. Chem.* **88**, 997 (1984); *Z. Wilhelm-Pieck-Universität, Rostock* **33**, 34 (1984).
- ²³D. M. Ceperley and H. J. Partridge, *J. Chem. Phys.* **84**, 820 (1986).
- ²⁴P. B. Foreman, P. K. Rol, and K. P. Coffin, *J. Chem. Phys.* **61**, 1658 (1974).
- ²⁵Note that this problem does not occur in the case of an electron gas with a Coulomb bare potential between its particles, for $dv(r)/dr$ is proportional to r^{-2} and the term $[\sin(kr) - kr \cos(kr)]$ goes to zero like r^3 as r goes to zero.
- ²⁶E. Feenberg, *Theory of Quantum Fluids* (Academic, New York, 1969).
- ²⁷R. B. Hallock, *J. Low Temp. Phys.* **9**, 109 (1972).
- ²⁸E. K. Achter and L. Meyer, *Phys. Rev.* **188**, 291 (1969).
- ²⁹M. Viviani, E. Buendia, A. Fabrocini, and S. Rosati, *Nuovo Cimento D* **8**, 561 (1985).
- ³⁰G. D. Buchan and R. C. Clark, *J. Phys. C* **10**, 3069 (1977).
- ³¹R. Scherm *et al.*, *Phys. Rev. Lett.* **59**, 217 (1987).
- ³²G. Sposito, *J. Low Temp. Phys.* **3**, 491 (1970).
- ³³G. D. Mahan, *Many Particle Physics* (Plenum, New York, 1990).
- ³⁴J. M. Farrar and Y. T. Lee, *J. Chem. Phys.* **56**, 5801 (1972); A. L. Burgmans, J. M. Farrar, and Y. T. Lee, *ibid.* **64**, 1345 (1976).